Novel synthetic approach to creating PtCo alloy nanoparticles by reduction of metal coordination nano-polymers†

Mami Yamada,*[a] Masayuki Maesaka,[a] Masato Kurihara,[b] Masatomi Sakamoto[b] and Mikio Miyake*[a]

Received (in Cambridge, UK) 10th June 2005, Accepted 18th August 2005
First published as an Advance Article on the web 7th September 2005
DOI: 10.1039/b508182c

PtCo alloy nanoparticles with different metal elemental ratios (Pt/Co = 0.9, 1.6, 2.9, and 3.6) were prepared by a novel synthetic approach, using the transformation reaction of platinum^{IV}/cobalt tetracyanoplatinate metal coordination nano-polymers (Pt^{II}-CN-Pt^{IV}/Co) *via* a H_2 gas-phase reduction.

Fuel cells have many advantageous characteristics and excellent energy conversion efficiency, scarcely discharging any environmental pollutants.[1] They are expected to replace conventional combustion engines as the next generation general energy system; however, in order to develop practical applications, we must first develop a highly efficient nanoparticle[2] catalyst. As a concrete problem, when Pt nanoparticles are used as an anode catalyst in a fuel cell, their catalytic activity is reduced by the strong absorption of CO molecules existing in hydrocarbon-reformed gas.[3] One way to solve this problem is to make Pt nanoparticles alloyed with other metal elements,[4–7] *e.g.*, Ru, Ni, Mo, Co, Fe. If the procedure for synthesising Pt alloy nanoparticles, which controls their metal elemental composition more precisely, is properly exploited, they will exhibit long-term activity with improved CO tolerance. It should be noted that the PtCo alloy nanoparticles are expected to be applicable to not only an anodic catalyst as noted above, but also a cathodic one due to the onset of oxide formation which is shifted to more positive potentials for the alloying.

In this communication, we demonstrate a novel synthetic approach to creating PtCo nanoparticles by transforming platinum^{IV}/cobalt tetracyanoplatinate^{II} metal coordination nano-polymers (Pt^{II}-CN-Pt^{IV}/Co) through a gas phase reduction in H_2 atmosphere. The transformation process accompanies the reduction of the metal ions and the removal of the bridging CN ligands. Metal coordination polymers have a great advantage in that the various metal elements can be connected by an appropriate organic ligand with uniform composition.[8–10] The attempt to isolate metal coordination polymers "on a nanometer scale" is possible by using the reverse micelle technique reported in our previous paper.[11] In Pt^{II}-CN-Pt^{IV}/Co, Pt and Co ions are bridged in advance by an organic CN ligand with a regular elemental composition; therefore, the PtCo nanoparticles obtained after the transformation hold a uniform dispersion of the metal constituents with the same elemental ratio as the precursor Pt^{II}-CN-Pt^{IV}/Co. We present the practical transformation process of Pt^{II}-CN-Pt^{IV}/Co into PtCo nanoparticles, in addition to the metal elemental control of Pt^{II}-CN-Pt^{IV}/Co reflecting on the transformed PtCo nanoparticles.

Pt^{II}-CN-Pt^{IV}/Co with different metal ratios were basically synthesized by mixing two transparent reverse micelle solutions, each of which was prepared from 2 mL of 0.4 M polyethylene glycol mono 4-nonylphenyl ether (NP-5: $HO(CH_2CH_2O)_n$-$C_6H_4C_9H_{19}$, $n = 5$)/cyclohexane with addition of 70 μL of 0.1 M aq. $K_2[Pt^{II}(CN)_4]$ and 0.1 M aqueous mixed solution of $Co^{II}Cl_2$ and $K_2Pt^{IV}Cl_6$ ($Co^{II} : Pt^{IV}$ = 1 : 0 (**1**), 2 : 1 (**2**), 1 : 1 (**3**), 1 : 2 (**4**)). After 3 h stirring, stearylamine (SA) 5 eq. to all of the included metal constituents (Pt and Co) was added to the reaction mixture and vigorously stirred for another 1 h, followed by the addition of methanol (*ca.* 50 ml) sufficient to deposit a slurry product on the bottom of the sample tube with a centrifuge. The finally filtered precipitate was washed sufficiently with methanol, and dried overnight in vacuum at room temperature to give a quantitative compound. The transformation reaction of Pt^{II}-CN-Pt^{IV}/Co was also performed after supporting on SiO_2 (5 wt% of Pt and Co). Pt^{II}-CN-Pt^{IV}/Co and SiO_2 were mixed in THF for 1 h. Then, the solvent was removed, and the product dried overnight in vacuum at rt to give SiO_2-supported Pt^{II}-CN-Pt^{IV}/Co. The prepared SiO_2-supported Pt^{II}-CN-Pt^{IV}/Co was reduced in a circular furnace in H_2 atmosphere (N_2/H_2 = 10, the total gas flow rate is 330 mL/min). The furnace temperature was raised at a rate of 10 °C/min, and kept at the prescribed temperature (350–450 °C) for 1–7 h. After the reaction, the furnace was cooled down naturally to room temperature. The obtained compounds were sealed in a sample tube in the N_2 atmosphere.

Compounds **1–4** of Pt^{II}-CN-Pt^{IV}/Co were obtained as a pale yellow powder, which can be dispersed in a less-polar solvent *e.g.*, THF, cyclohexane with a surface active agent. The XPS spectra of **1–4** exhibited several signals attributed to Co2p (781.9 eV), N1s (402.4 eV), Pt4d (320.5, 337.6 eV), and C1s (284.5 eV). The metal elemental ratios of **1–4** determined by EDX analysis are summarized in Table 1, indicating that the ratio of the metal

Table 1 Pt/Co ratio and the lattice constant of compounds **1–4**

Compound	Pt/Co (cal.)[a]	Pt/Co (anal.)[b]	Lattice constant *a* (Å)[c]
1	1	0.9	3.76
2	2	1.6	3.83
3	3	2.9	3.86
4	5	3.6	3.88

[a] The mixed ratio of the starting complexes. [b] Determined by EDX. [c] Calculated from the XRD results.

[a]*Department of Physical Materials Science, Japan Advanced Institute of Science and Technology (JAIST), 1-1 Asahidai, Nomi-shi, Ishikawa, 923-1292, Japan. E-mail: myamada@jaist.ac.jp; miyake@jaist.ac.jp; Fax: +81-761-51-1116; Tel: +81-761-51-1540*
[b]*Department of Biological Chemistry, Faculty of Science, Yamagata University, 1-4-12 Kojirakawa, Yamagata, 990-8560, Japan*

† Electronic supplementary information (ESI) available: TEM images, IR spectra analysis, XRD patterns, TGA curve, XPS spectra, and IR spectra of the compounds. See http://dx.doi.org/10.1039/b508182c

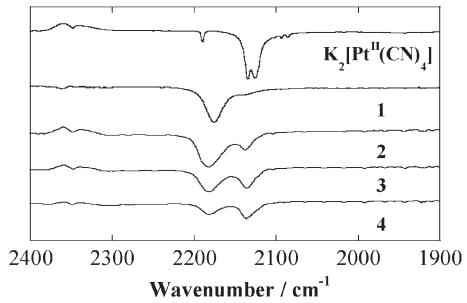

Fig. 1 IR spectrum of $K_2[Pt^{II}(CN)_4]$ and compounds **1–4**.

components in Pt^{II}-CN-Pt^{IV}/Co is controllable by adjusting the molar ratio of the starting metal complexes in the reaction mixture. The TEM images of **1–4** confirmed that spherical particles of Pt^{II}-CN-Pt^{IV}/Co with a diameter of *ca.* 15 nm were formed (Electronic Supplementary Information, Fig. S1). As for the FT-IR spectra of **1–4**, ν(NH) at 1468 cm^{-1} and ν(CH) at 2922 cm^{-1} and 2850 cm^{-1} of the attached SA were observed. The broad peaks at 2180 cm^{-1} and 2137 cm^{-1} can be assigned to ν(CN) of the Pt^{II}-CN-Co^{II} and Pt^{I}-CN-Pt^{IV} unit, respectively; the value was shifted to a higher energy region compared to the starting $K_2[Pt^{II}(CN)_4]$ complex (Fig. 1). This result supports the complexation of $Pt^{II}(CN)_4^{2-}$ with Co^{2+} and Pt^{4+}cations through the bridging CN ligands of $Pt^{II}(CN)_4^{2-}$.[11–13] The variation in the intensity rate between the CN stretching caused by the Pt^{II}-CN-Co^{II} and the Pt^{II}-CN-Pt^{IV} units is reasonably related to the metal elemental ratio in the compound, supporting the EDX results (Fig. S2).

TGA analysis of **1** under H_2 atmosphere revealed that the removal of the CN ligands occurred from 350 to 450 °C with a weight loss of 24%, which was consistent with the calculated value of 29% (Fig. S3). Within this temperature region, the precise transformation condition of **1** to PtCo nanoparticles was first explored with a different reaction time. The XPS spectra of **1** before and after the gas-phase reduction at 350 °C showed that when the reaction time was increased, the Pt4f signals at 73.1 eV and 76.4 eV decreased in intensity, while new signals appeared at 71.2 eV and 74.5 eV due to the metal Pt (Fig. 2, left).[14] Additionally, the intensity of the CN stretching signal of **1** in an IR spectrum was also reduced with increasing reaction time (Fig. S4). These findings led us to deduce that the transformation reaction of **1** gradually occurs in practice by the reduction of Pt and Co ions accompanied by the removal of the bridging CN ligands, and the transformation extent becomes larger with increasing reaction time. On the other hand, with a fixed reaction time of 3 h, the higher reaction temperature led to a larger ratio of the metal Pt in the compound (Fig. 2, right). Co ions are also converted to Co^0 in the conditions where Pt ions are reduced to Pt^0, which was confirmed by the Co2p signals (Fig. S5). By considering the intensity ratio of the newly appeared peaks (Pt^0) to the original ones (Pt^{II}-CN-Pt^{IV}) in the Pt4f energy region of the XPS spectra, it is confirmed that the transformation reaction of **1** was fully completed at 400 °C within 3 h.

Fig. 3 shows the XRD patterns of compounds **1–4** after the transformation reaction at 400 °C for 3 h. They exhibit a typical fcc structure entirely different from the pattern before the reaction (Fig. S6). The diffraction peaks in the pattern of **1** (anal. Pt/Co = 0.9) and **3** (anal. Pt/Co = 2.9) after the transformation reaction were consistent with those in the JCPDS data of PtCo and Pt_3Co, respectively.[15] In the XRD patterns, the diffraction peaks are shifted to lower diffraction angles almost linearly with an increase of the Pt component in the compound (Vegard's law). When a Pt atom on a Pt site is replaced by a Co atom with a smaller radius, the lattice constant, *a*, will decrease (Table 1). These findings clearly indicate that the metal components are well dispersed in an alloy nanoparticle; this can be attributed to the merit of this method, that the metal units are uniformly scattered beforehand in Pt^{II}-CN-Pt^{IV}/Co by connection of an organic ligand.

In the TEM images of SiO_2-supported **1–4** after the transformation reaction, most particles have a below 10 nm diameter, except for some large particles beyond 15 nm diameter due to particle aggregation; the main particle size is apparently reduced compared to that of Pt^{II}-CN-Pt^{IV}/Co (Fig. 4). In compound **1**, the estimated length of the Pt-CN-Co unit in Pt^{II}-CN-Co is 5.28 Å, while the distance between a Pt and Co atom is 3.82 Å.[16] The shrinkage rate

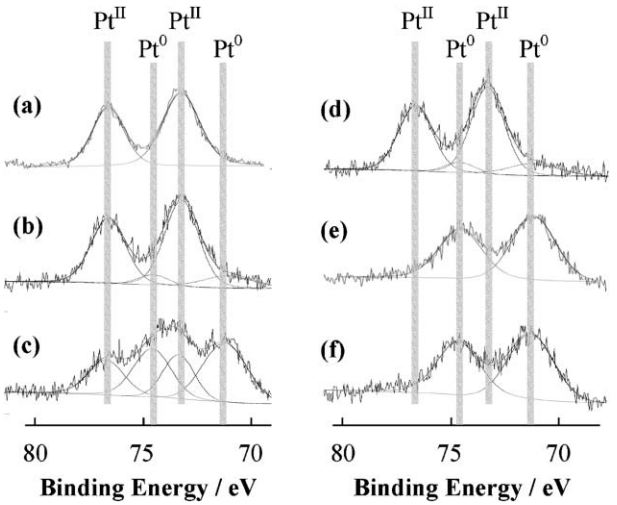

Fig. 2 XPS curve in the Pt4f energy range of compound **1** before (a) and after the transformation reaction in H_2 atmosphere at 350 °C for 3 h (b)(d), at 350 °C for 5 h (c), at 400 °C for 3 h (e), and at 450 °C for 3 h (f) .

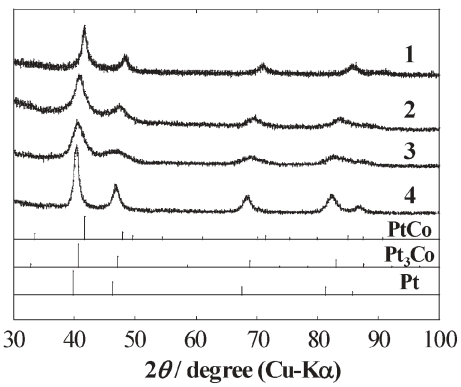

Fig. 3 XRD patterns of compounds **1–4** after the transformation reaction in H_2 atmosphere at 400 °C for 3 h with JSPDS data of PtCo, Pt_3Co, and Pt. The diffraction points can be indexed as (111), (200), (220), and (311) reflections of fcc.

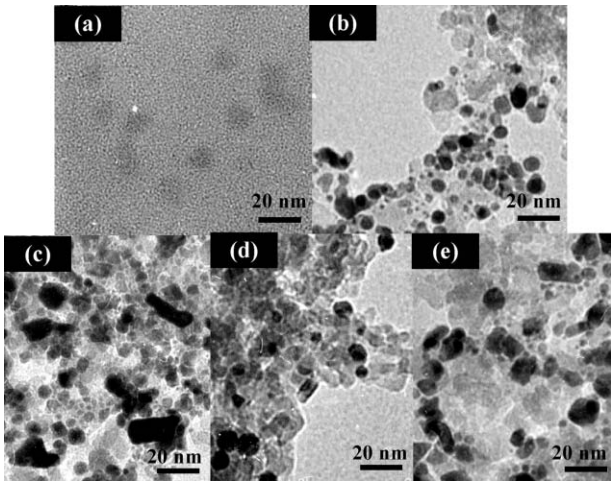

Fig. 4 TEM images of compound **1** (a) and compounds **1–4** after the transformation reaction in H_2 atmosphere at 400 °C for 3 h (b, c, d, and e, respectively).

of the particle diameter before and after the transformation process is calculated as 0.72, which value is agreeable with the observed value, 10 nm/15 nm = *ca.* 0.7. Particles with a less than 5 nm diameter can also be observed, which might be produced by the physical division of a single particle during the transformation process, especially the removal of the CN ligand. The catalytic activity of the prepared PtCo alloy metal nanoparticles is under investigation in our laboratory.

In conclusion, we have described the novel preparation of platinum^{IV}/cobalt tetracyanoplatinate^{II} metal coordination nanopolymers (Pt^{II}-CN-Pt^{IV}/Co) protected by an alkyl ligand of stearylamine using a reverse micelle technique. The metal elemental control of Pt^{II}-CN-Pt^{IV}/Co could be attempted by changing the ratio of the starting complexes. The complete conversion of Pt^{II}-CN-Pt^{IV}/Co to PtCo alloy metal nanoparticles was performed by a H_2 gas-phase reduction above 400 °C for 3 h, accompanied by the removal of the bridging CN ligand. The metal elemental ratio was maintained before and after the transformation reaction. We have begun exploring applications of this method for preparing other kinds of alloy metal nanoparticles (PtRu, PtFe, PtCoFe, *etc.*), along with the simultaneous investigation of their catalytic activity. Some synthetic parameters, *e.g.* the micelle concentration, the water droplet size in a reverse micelle solution, the reducing method (liquid phase), the ratio of metal loading to supports, and the supporting matrix (carbon matrix which is generally used for a fuel cell) also should be considered for the generation of smaller catalytic particles useful for a practical fuel cell. We believe that this novel approach to the synthesis of alloy metal nanoparticles will widen the techniques of nanomaterial architecture.

This work was supported by Grants-in-Aid for Scientific Research (No. 1610069), Center of Excellence (COE) Program from the Ministry of Culture, Education, Sports, Science and Technology, Japan.

Notes and references

1 A. K. Shukla, P. A. Christensen, A. Hamnett and M. P. Hogarth, *J. Power Sources*, 1995, **55**, 87.
2 M.-C. Daniel and D. Astruc, *Chem. Rev.*, 2004, **104**, 293.
3 K. V. Kordesch, G. Onter and R. Simader, *Chem. Rev.*, 1995, **97**, 191.
4 Z. Liu, J. Y. Lee, W. Chen, M. Han and L. M. Gan, *Langmuir*, 2004, **20**, 181.
5 L. Xiong and A. Manthiram, *J. Mater. Chem.*, 2004, **14**, 1454.
6 S. Scaccia and B. Goszczynska, *Talanta*, 2004, **63**, 791.
7 A. E. Russell and A. Rose, *Chem. Rev.*, 2004, **104**, 4613.
8 J. Veciana, C. Rovira and D. B. Amabilino, *Supramolecular Engineering of Synthetic Metallic Materials*, Kluwer Academic Pub., Indiana, 1998.
9 S. Ferlay, T. Mallah, R. Ouahés, P. Vellet and M. Verdaguer, *Nature*, 1995, **378**, 701.
10 N. Shimamoto, S. Ohkoshi, O. Sato and K. Hashimoto, *Inorg. Chem.*, 2002, **41**, 678.
11 M. Yamada, M. Arai, M. Kurihara, M. Sakamoto and M. Miyake, *J. Am. Chem. Soc.*, 2004, **126**, 9482.
12 N. Kondo, A. Yokoyama, M. Kurihara, M. Sakamoto, M. Yamada, M. Miyake, T. Ohsuna, H. Aono and Y. Sadaoka, *Chem. Lett.*, 2004, **33**, 1182.
13 K. Nakamoto, *Infrared and Raman Spectra of Inorganic and Coordination Compounds*, John Wiley & Sons, Inc., U. S. A., 1986.
14 J. F. Moulder, W. F. Stickle, P. E. Sobol and K. D. Bomben, *Handbook of X-Ray Photoelectron Spectroscopy*, Perkin Elmer, U. S. A., 1992.
15 Note that the metal elemental ratio of the compounds was maintained before and after the transformation reaction as confirmed by EDX.
16 P. Yu, M. Pemberton and P. Plasse, *J. Power Sources*, 2005, **144**, 11.